Proceedings of the 5th International Conference on Modern Medicine and Global Health
DOI: 10.54254/2753-8818/2027.39310

Single/Double Degree-of-Freedom Switching Mechanism and Performance Verification of a Reconfigurable Quadruped Wheeled Robot

Yutian Cai

School of Mechanical and Electrical Engineering & Automation, Xiamen University Tan Kah Kee College, Zhangzhou, China
CYT2156@outlook.com

Abstract. In this paper, a quadrupedal wheeled robot with reconfigurable single- and double-degree-of-freedom (DOF) modes is proposed, which is accomplished by knee joint folding and the use of mechanical limiters, without requiring any additional locking components. The lower leg is folded against a mechanical stop and a holding torque is applied to restrict the leg to a single degree of freedom for flat ground wheeling, while the stop is released to allow the leg to move with two degrees of freedom in the hip and knee for legged obstacle traversal. Kinematic and finite element models are created, and MuJoCo simulations are performed using a unified robot description format (URDF) model, which uses reinforcement learning to generate walking gaits. The double-DOF mode increases the maximum foot span by 24% (to 0.411 m) and provides 41% more clearance in the vertical direction, and the workspace changes from a one-dimensional arc to a two-dimensional (2D) area. The chassis, joint output shafts and limiters are not stressed beyond their material yield strengths with rated payloads of 20 kg and safety factors of 2.7–4.0. The robot was able to complete the five 20 s trials without falling, making a journey of approximately 1.94 m with an average speed of 0.098 m/s, and peak joint torques that were within the 25 N·m limit. These results confirm the kinematic and simulation feasibility of the mechanism, while prototype validation of repeated switching, load holding, and actual obstacle traversal remains to be completed.

Keywords: quadruped wheeled robot, reconfigurable mechanism, single/double degree-of-freedom switching, mechanical limit, dynamic simulation

1. Introduction

Wheeled mobile robots are known to have high efficiency, low energy consumption, and simple control on flat surfaces; however, they have difficulties in overcoming obstacles and adapting to unstructured surfaces. Legged robots have the advantage of discrete foot placement to help them move over obstacles and adjust to various terrain conditions, but their disadvantages include energy efficiency, slow movement speed and difficulty in control. Wheel-leg (Wheg)-based hybrid robots are also an important research direction in mobile robotics, which integrate both types of mobility in

© 2026 The Authors. This is an open access article distributed under the terms of the Creative Commons Attribution License 4.0 (https://creativecommons.org/licenses/by/4.0/).

DOI: 10.54254/2753-8818/2027.39310

one platform, combining the two mechanisms: wheels and legs. How to transfer the same leg mechanism to achieve the different degree of freedom in different terrains, however, is still a challenge in the design of such robots [1, 2].

The current leg-wheel hybrid robots have almost fixed setting of the hybrid parts such as the number of degrees of freedom of legs and the integration method of legs and wheels, which is hardly changeable after the robot is designed. Current reconfigurable and modular robots can change their configuration by combining modules or by switching states, but they either do not allow continuous operation because of the need for manual disassembly and reassembly of modules or require the addition of extra locking devices, such as clutches or electromagnetic locks, to secure the joint to increase the complexity of the mechanism, weight and potential failure points [3-6]. Though these added locks make it easier to control, they also somewhat negate the compactness benefits of reconfigurable designs.

The purpose of this paper is to realize online switching between one degree of freedom and two degrees of freedom with the same leg mechanism without increasing additional locking components. For this purpose, two questions are worth answering: (1) Is it possible to geometrically fix and develop a configuration, even when the lower leg is folded to the mechanical end position? (2) How much does the motion range of the foot-end differ between single- and double-degree-of-freedom configurations and what is the dynamic feasibility of the switching mechanism?

The main contributions of this paper are the design of the leg mechanism with direct drive from the knee-joint motor and the adoption of mechanical constraints at the thigh root to switch between the single degree of freedom and two degree of freedom configurations, which share the end effector (foot) between wheels and legs without using any extra locking devices; kinematic models of the two configurations are established, and reachable foot workspace is compared; static strength finite element analyses of the body frame, output shafts of knee and hip joints and the limit components are conducted; dynamic simulations are performed based on the unified robot description format (URDF) model in MuJoCo, and the reinforcement learning strategies are implemented to generate walking gaits; results on joint torques, forward velocity and attitude stability are obtained, which preliminarily verifies the dynamic feasibility of the mechanism.

The rest of this paper is organized as follows: The reconfigurable mechanism, modeling and simulation methods are presented in Section 2; the simulation results on working volume, structural strength and dynamics are given in Section 3; the performance trade-offs and research limitation are discussed in Section 4; and a summary of the paper is provided in Section 5.

2. System design and research methodology

2.1. Reconfigurable mechanism and switching method

The main body of the robot has a frame-type load-bearing structure and is located in the middle of the four legs, which are symmetrically arranged in a symmetrical structure. Both legs are in a hip-knee serial configuration in which the hip and knee joints are directly driven by motors. The foot end is also a wheel-foot mechanism, where the wheels also act as the walking feet. In the single-degree-of-freedom (DOF) configuration (Figure 1(a)), the motor of the knee joint folds the lower leg backward, but when the lower leg reaches the mechanical stop surface at the base of the thigh, the motor switches to a torque holding mode to hold the lower leg against the mechanical stop. Thus, the lower and upper legs are similar to a rigid link, and the end-wheel rolls on the flat surface while only the hip joint is free to move. During the dual-degree-of-freedom configuration (Figure 1(b)), the knee joint comes out of the holding phase and moves the lower leg away from the stop position

DOI: 10.54254/2753-8818/2027.39310

to allow coordinated action between the hip and knee joints for stepping and obstacle traversal of the foot end. The control process involved in the configuration switching is a "folding into place—torque holding—state confirmation": When switching to the lower leg configuration, position control is used to fold the lower leg; upon detecting contact through the current signal threshold and the joint encoder, the system enters the holding mode; when switching to the unfolding configuration, the leg encoder is used to confirm that the lower leg has left the stop surface. It is all direct motor drive with mechanical stops; no clutches or electromagnetic locks. The stop parts are made from tempered 40Cr steel and the contact surfaces are fitted with polyurethane buffer pads that help to dampen impact and noise while folding.

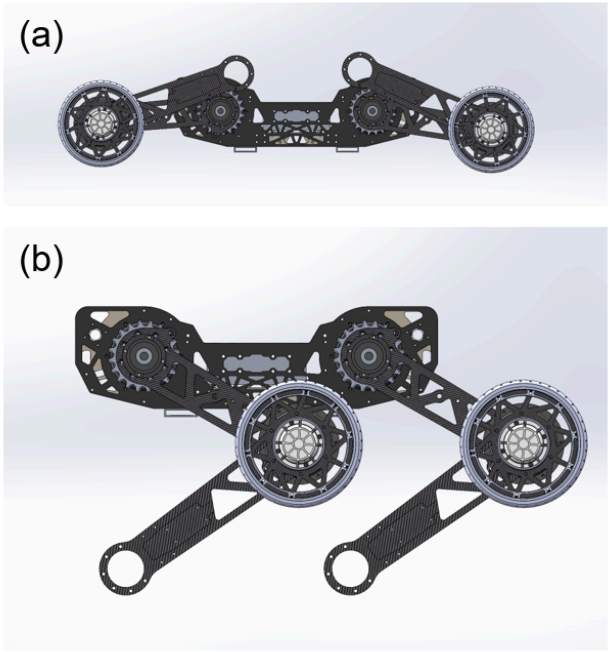


Figure 1. Single/double degree-of-freedom configurations: (a) single degree of freedom (lower leg folded to the mechanical limit and held); (b) double degree of freedom (knee joint released with coordinated hip-knee motion)

2.2. Kinematic modeling and strength analysis

In the leg motion plane, a kinematic model is built by the Denavit-Hartenberg (DH) parameter method. If the hip joint is taken as the origin, the length from hip to thigh as l_1 and length from knee to foot as l_2, the angle at the hip joint as θ_1 and the angle at the knee joint as θ_2, then the foot end position satisfies

$$x = l_1 \cos\theta_1 + l_2 \cos(\theta_1 + \theta_2), \quad z = l_1 \sin\theta_1 + l_2 \sin(\theta_1 + \theta_2) \tag{1}$$

For the two-degree-of-freedom configuration, both θ_1 and θ_2 are allowed to range within the limits of their respective joints; in the single-degree-of-freedom configuration, the knee joint is locked at the folded angle, $\theta_2 = \theta_{limit}$, and the model is reduced to a single-link pendulum, with the foot end moving along an arc centered at the hip joint and with a radius equal to the folded envelope length. Using this model, dense sampling in the joint ranges will enable the reachable foot end

DOI: 10.54254/2753-8818/2027.39310

regions to be determined for both configurations and performance measures, like maximum stride width and vertical range of motion, to be calculated.

Static finite element analysis was used to verify the structural strength. The body, the joint output shaft, and the limit components were modeled as 6061-T6 aluminum alloy, 7075-T6 aluminum alloy and 40Cr steel respectively. Fixed constraints were given to the mounting conjuncture surface of the body and the joint housing, and a load was applied to the load-bearing surface in the analysis, which is the rated load of 20 kg, plus the self-weight of the component. Meshing was performed by solid elements and local refinement around the areas of high stresses such as contact surfaces of limiters and shoulder areas of shafts. The maximum equivalent stress and maximum deformation of each component were output.

2.3. Dynamic simulation and strategy

To test the feasibility of the mechanism in dynamic walking, a dynamic simulation was created using MuJoCo physics engine based on the URDF model [7]. The model contains four legs, for a total mass of approximately 10.59 kg, with eight actuated independent joints at the hips and knees with a maximum torque of 25 N·m, and the simulation is run with a physical time step of 0.002 s. The policy produces 8 target offsets of joint angle every 0.02 s and is controlled by a proportional-derivative (PD) control law.

$$\tau = 45(q_{target} - q) - 2\dot{q} \tag{2}$$

Determine actuating torque and use limiting [8]. The locomotion strategy is learned using Proximal Policy Optimization (PPO) and observations consist of body velocity, body orientation, target velocity, joint velocity, joint position, etc. The objective is to accelerate towards the goal at a velocity of 0.15 m/s [9, 10]. Evaluation is conducted while the body is set at standing height: several episodes are repeated and forward displacement, velocity, posture of the body, state of the feet and actuating torques of the joints are recorded; if a fall occurs or if non-foot parts touch the ground an episode is deemed to be impossible and the test is repeated. Note that PD gains, friction and inertia parameters are extracted from URDF and initial simulation values, and thus the results are used for comparing to validate the simulation feasibility of the mechanism and not directly to performance in the real world.

3. Results

3.1. Workspace comparison of single- and double-degree-of-freedom

Using the method described in Section 2.2, the reachable areas of the foot end for both configurations were computed and presented in Figure 2. With the two-degree-of-freedom configuration the foot end is capable of sweeping a two-dimensional (2D) band-like area, resulting in a reachable area of about 0.029 m^2 using grid-based statistics within the joint ranges. The knee joint is locked in the single degree of freedom configuration, which means that the foot end can only move along a circular arc of length approximately 0.577 m, which is a one-dimensional reachable range. Through quantitative comparison, it is shown that the maximum stride width of the two-degree-of-freedom configuration can be increased to 0.411 m, which is about 24% larger than that of the single-degree-of-freedom configuration (0.331 m). The vertical reach of the foot end is improved from 0.196 m in the single degree of freedom case to 0.276 m, an increase of approximately 41%.

DOI: 10.54254/2753-8818/2027.39310

The maximum reachable height of the foot end from the ground for the two-degree-of-freedom configuration is about 0.258 m for the body at standing height. Stride width and vertical reach is increased by the foot end, after releasing the knee joint, spreading out from a fixed arc to a 2D region. It is important to note that the above values of height and stride are obtained by kinematic geometric modeling and are not actual values obtained during obstacle crossing experiments.

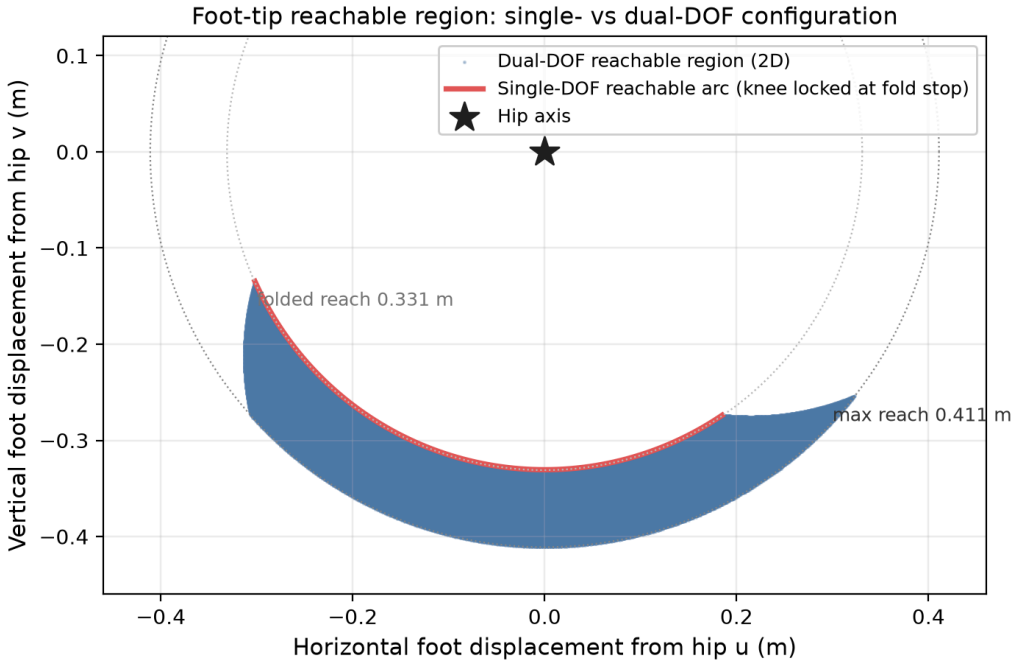


Figure 2. Two-dimensional reachable area of the double-degree-of-freedom configuration (blue) compared with the reachable arc of the single-degree-of-freedom configuration (red)

3.2. Structural strength analysis results

The maximum equivalent stress for each of the body, the joint output shaft and the limit components was determined after the static analysis in Section 2.2, and it was confirmed that the maximum equivalent stress was not greater than the yield strength of the material. The safety factor, defined as the ratio between material yield strength and the maximum equivalent stress, was about 2.7 to 4.0. In static load condition with a rated load of 20 kg, none of the three critical load bearing components were subjected to loads beyond the yield strength of the materials. These results are only valid for static loading conditions as described in this study and do not apply to repeated impacts, fatigue or power-loss retention performance.

3.3. Walking results of dynamic simulation

The learned walking policy was tested as outlined in Section 2.3. During five 20 s simulations the robot did not fall, and no non-foot contact occurred, the robot moving forward a distance of 1.938–1.941 m (the steady state forward velocity after 2 s being approximately 0.098 m/s). The minimum vertical cosine of body orientation was ~0.994 with forward displacement of ~0.969 m and lateral displacement of ~0.052 m for a playback of 10 s. The gait sequence is shown in Figure 3. All foot ends showed overlapping support and lift-off phases, but the support ratios of front and hind legs

DOI: 10.54254/2753-8818/2027.39310

were not balanced (roughly 0.62–0.88) and there were problems like jittering of the feet, low lifting of the legs and slipping, which are typical of a slow-start gait.

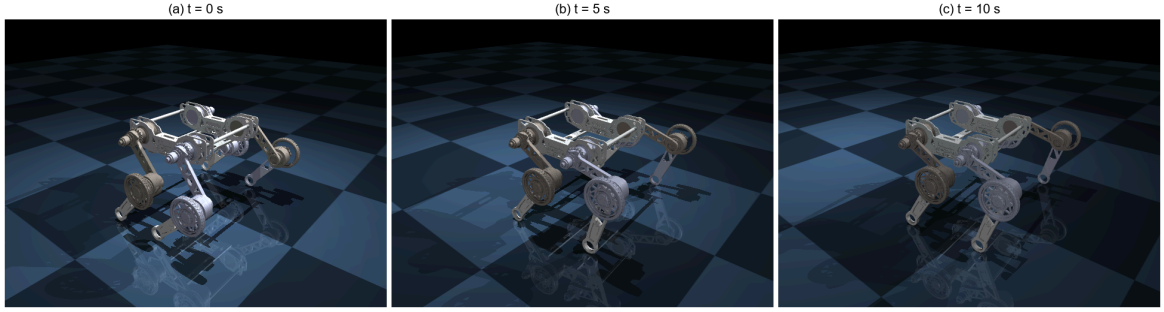


Figure 3. Dynamic simulation gait sequence for the two-degree-of-freedom configuration at (a) t = 0 s, (b) t = 5 s, and (c) t = 10 s

The actuating torque of the eight joints during walking is illustrated in Figure 4 and the peak value and root-mean-square (RMS) value are included in Table 1.

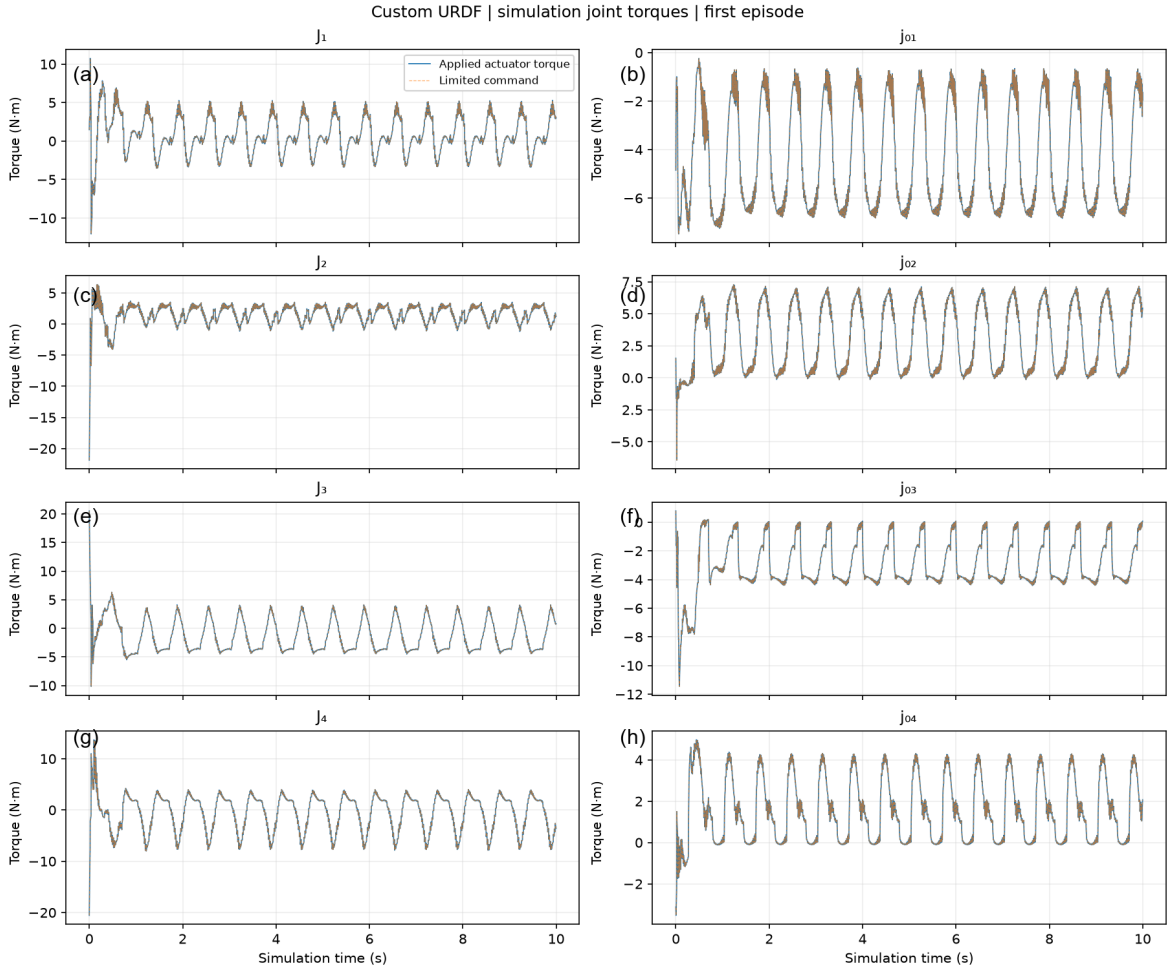


Figure 4. Actuating torque of the eight joints in the first trial for the two-degree-of-freedom configuration: (a) J1, (b) j01, (c) J2, (d) j02, (e) J3, (f) j03, (g) J4, and (h) j04 (blue line: actuating torque; orange dashed line: clamped command)

DOI: 10.54254/2753-8818/2027.39310

Table 1. Peak and root-mean-square actuating torque of the eight joints during walking simulation

Joint	Peak torque (N·m)	Root-mean-square torque (N·m)	Joint	Peak torque (N·m)	Root-mean-square torque (N·m)
J_1	12.16	2.50	J_3	20.75	3.11
j_{01}	7.48	4.84	j_{03}	11.45	3.42
J_2	21.90	2.22	J_4	20.57	3.57
j_{02}	7.37	3.97	j_{04}	5.20	2.18

The peak joint torques vary from 5.20 to 21.90 N·m and are lower than 25 N·m among which the hip joints (J_1–J_4) have greater peak values (12.16–21.90 N·m) and the knee joints (j_{01}–j_{04}) have root mean square values of about 2.18–4.84 N·m. The results show that joint torques do not exceed the limits defined by the URDF under this slow gait, and that stable slow walking can be achieved in dynamic simulation. However, there are still some limitations, such as gait speed, leg-lift height, and uniformity of contact, and these results are based on the simulation parameters; the actual dynamic performance needs to be validated.

4. Discussion

4.1. Performance trade-offs of single- and double-degree-of-freedom

It shows that the available results suggest single-DOF and double-DOF configurations are suitable for different tasks. The former immobilizes the knee joint which makes the leg geometry more deterministic and closer to a wheeled configuration on flat ground; the latter makes the knee joint free, leading to a greater foot span and a larger two-dimensional reachable area, but the joint motion and control are more complex and allow for richer obstacle-crossing postures. Both configurations are not absolutely better or worse without consideration to the task requirements; the ability to change the configuration is what makes the difference when choosing mobility capabilities for flat-ground travel and obstacles negotiation. It should be pointed out that there are no experiments in this study performed with other reconfigurable schemes under exactly the same conditions to draw conclusions about the "simplest mechanism" or "highest reliability" of this design.

4.2. Mechanical limiting and motor holding

Although the folding limit can geometrically define a single-degree-of-freedom configuration, the retention of the configuration is still dependent on the direction of external loads, knee joint holding torque and the contact state of the limit. Whether the knee joint has to produce a holding torque all the time or whether the knee remains locked on power loss, or whether reverse loads would cause the lower leg to come away from the limit is not known. If the impact force is repeatedly applied to the limit, it also causes shock and wear. Current static strength results only suggest that parts will not instantly fail when loaded beyond their strength, but their results cannot be used to verify stable operation when subject to other stresses like power-off retention, long term temperature rise, repeated impact, wear, etc.

DOI: 10.54254/2753-8818/2027.39310

4.3. Inadequate testing and future research needs

Mechanism design, kinematic results, static strength analysis and dynamic simulation have been provided in the current work, but performance at prototype level, such as repeated switching, load-holding capability and operation in real terrain still have to be supplemented. Next, it may be necessary to measure the multiple switching times and the number of successful switches, then verify configuration retention at rated load and power off, and then try demonstration of the real capability of the dual degree of freedom configuration with different height obstacles and different loads. At the same time, impact, mechanical limits wear and temperature increase during knee joint holding for long periods of time should also be considered. When a time limit is available, the tests corresponding to the two fundamental requirements of the design – "ability to switch" and "ability to maintain after switching" – that is, for repeated switching time and for load-holding time, should be performed first.

5. Conclusion

In this paper, the quadruped wheeled robot mechanism which can switch between single-DOF and dual-DOF modes by knee joint folding and position limiting is presented. URDF-based kinematic models are created for both configurations and finite element models are created for some of the load-bearing components, with dynamic simulations being performed in MuJoCo. Given the structural parameters, the knee joint is released to extend a one-dimensional (1D) arc of the foot end into a 2D workspace, which will increase the maximum stride width from 0.331 m to 0.411 m and the vertical range by about 41%. The single degree of freedom configuration, on the other hand, results in a more deterministic leg geometry with locked knee joint. With static analysis at a rated load of 20 kg, the chassis, output shaft and limiting components are all within their respective material yield strengths. The results of the dynamic simulation indicate that the robot is able to walk at a slow speed around 0.098 m/s, and the joint torques are still in the allowable range. It should be noted that the dynamic results are based on simulation; the data for repeated configuration switching, load-holding performance, power-off, long-term temperature rise, and real-world obstacle traversal is incomplete. So, at this point, only the feasibility of the mechanism design and simulation results can be certified, and it cannot be concluded that the long-term reliability or performance on complex terrain has been fully verified. Future research should focus on experiments with more than one configuration switch and load holding tests, but also the testing and analysis of impact forces, wear and temperature increase for long holding of knee joint under different loads under the condition of dual-degree-of-freedom configuration.

References

[1] Niu, J., Wang, H., Shi, H., Li, D., Li, S., & Wu, S. (2017). Trajectory planning verification and gait analysis of wheel-legged hybrid robot with variable degree of freedom. *Transactions of the Chinese Society of Agricultural Engineering, 33*(23), 38–47. https://doi.org/10.11975/j.issn.1002-6819.2017.23.006

[2] Liu, Y. (2021). Design and implementation of compound wheel-footed robot. Southwest University, Chongqing. https://doi.org/10.27684/d.cnki.gxndx.2021.001188

[3] Zhang, X. (2025). Design of transformable wheel-leg structure for mobile robots and study on multi-terrain motion characteristics. Yantai University, Yantai. https://doi.org/10.27437/d.cnki.gytdu.2025.000479

[4] Zhao, J. (2023). Structural design and mechanical analysis of a wheel-leg hybrid magnetic adhesion wall-climbing robot. Hebei University of Technology, Tianjin. https://doi.org/10.27105/d.cnki.ghbgu.2023.000387

[5] Bjelonic, M., Bellicoso, C. D., de Viragh, Y., Sako, D., Tresoldi, F. D., Jenelten, F., & Hutter, M. (2019). Keep rollin'—whole-body motion control and planning for wheeled quadrupedal robots. *IEEE Robotics and Automation*

DOI: 10.54254/2753-8818/2027.39310

Letters, 4(2), 2116–2123. https://doi.org/10.1109/LRA.2019.2899750

[6] de Viragh, Y., Bjelonic, M., Bellicoso, C. D., Jenelten, F., & Hutter, M. (2019). Trajectory optimization for wheeled-legged quadrupedal robots using linearized ZMP constraints. *IEEE Robotics and Automation Letters, 4*(2), 1633-1640. https://doi.org/10.1109/LRA.2019.2896721

[7] Chamorro, S., Klemm, V., de la Iglesia Valls, M., Pal, C. J., & Siegwart, R. (2024). Reinforcement learning for blind stair climbing with legged and wheeled-legged robots. *Proceedings of the 2024 IEEE International Conference on Robotics and Automation (ICRA)*, Yokohama, Japan, 8081-8087. https://doi.org/10.1109/ICRA57147.2024.10610069

[8] Teixeira de Paula, D., Godoy, E. P., & Becerra-Vargas, M. (2024). Dynamic modeling and simulation of a torque-controlled spatial quadruped robot. *Robotica, 42*(8), 2761-2780. https://doi.org/10.1017/S0263574724001097

[9] Alvarez-Padilla, J., Zhang, J. Z., Kwok, S., Dolan, J. M., & Manchester, Z. (2025). Real-time whole-body control of legged robots with model-predictive path integral control. *Proceedings of the 2025 IEEE International Conference on Robotics and Automation (ICRA)*, Atlanta, GA, USA, 14721-14727. https://doi.org/10.1109/ICRA55743.2025.11128271

[10] Mohseni, O., Davoodi, A., Ahmadi, A., Firouzi, V., Nasiri, R., & Ahmadabadi, M. N. (2022). Coupling of body mechanics and control for robust and efficient quadrupedal gait generation. *Proceedings of the 2022 10th RSI International Conference on Robotics and Mechatronics (ICRoM)*, Tehran, Iran, 29-35. https://doi.org/10.1109/ICRoM57054.2022.10025267